

# Angle-resolved photoelectron spectroscopy study of the anion-derived dangling-bond band on ZnO(10 $\bar{1}$ 0)

K. Ozawa,\* K. Sawada, Y. Shirotori, and K. Edamoto

*Department of Chemistry and Materials Science, Tokyo Institute of Technology, Ookayama, Meguro-ku, Tokyo 152-0033, Japan*M. Nakatake<sup>†</sup>*Institute of Materials Structure Science, High Energy Accelerator Research Organization, Tsukuba, Ibaraki 305-0801, Japan*

(Received 22 May 2003; published 26 September 2003)

The band structure of surface electronic states on the ZnO(10 $\bar{1}$ 0) surface has been investigated by angle-resolved photoelectron spectroscopy utilizing synchrotron radiation. Photon-energy dependent measurement and the K and O<sub>2</sub> adsorption studies have been carried out to identify the surface-localized O 2*p* dangling-bond state. It is found that the state exists at 3.7 eV below the Fermi level at the  $\bar{\Gamma}$  point in the surface Brillouin zone and shifts to the higher binding-energy side by 0.8 and 0.5 eV along the  $\bar{\Gamma}X$  and  $\bar{\Gamma}X'$  axes, respectively. The O 2*p* dangling-bond band is found to locate below the upper edge of the projected bulk bands along these two high-symmetry axes. The present study settles a controversial issue on the energetic position of the O 2*p* dangling-bond band, which has been in dispute among theoretical studies.

DOI: 10.1103/PhysRevB.68.125417

PACS number(s): 71.20.Nr, 73.20.At, 79.60.Bm

## I. INTRODUCTION

Zinc oxide (ZnO) is one of the most important oxide semiconductors because of a wide variety of its applications such as catalysts, chemical sensors, piezoelectric transducers, varistors, etc. Moreover, ZnO has been found to be a potential material for optoelectronic devices of blue light emitter and laser diode.<sup>1,2</sup> Therefore, understanding the bulk and surface electronic structures of ZnO is of particular importance in order to further explore the possibility of ZnO as industrially important materials.

ZnO crystallizes into the wurtzite structure, and the polar (0001)-Zn and (000 $\bar{1}$ )-O surfaces and the nonpolar (10 $\bar{1}$ 0) surface have been objects of experimental and theoretical studies. Of these surfaces, the nonpolar (10 $\bar{1}$ 0) surface is of particular interest from the view point of surface chemistry, because the surface is terminated with the same number of O and Zn atoms, i.e., the surface is covered with both Lewis acid and base sites. Figure 1 shows the structural model of ZnO(10 $\bar{1}$ 0). The surface is composed of the Zn-O dimer rows along the  $[1\bar{2}10]$  direction. The low-energy electron-diffraction (LEED) studies have revealed that the surface undergoes relaxation, which is characterized by downward shift of both surface Zn and O atoms with a greater shift for the Zn atom than the O atom, resulting in the Zn-O bond rotation by 6.2° (Ref. 3) or 11.5° (Ref. 4) with respect to the ideal surface plane. Such a surface relaxation should influence the energetic position as well as the dispersion width of the surface dangling-bond bands of the occupied O 2*p* and unoccupied Zn 4*s* states. Several theoretical studies have indicated that, upon relaxation, the O 2*p* dangling-bond state is stabilized while the Zn 4*s* dangling-bond state shifts up in energy.<sup>5,6</sup> However, the theoretically determined position of these dangling-bond bands, especially the occupied O 2*p* dangling-bond band, relative to the bulk bands projected onto the (10 $\bar{1}$ 0) surface varies depending on the method employed in the calculations.

Ivanov and Pollmann have used an empirical tight-binding method and found that the O 2*p* dangling-bond state lies just below the upper edge of the projected bulk bands on the unrelaxed ideal ZnO(10 $\bar{1}$ 0) surface.<sup>7</sup> The model calculations have predicted that the O 2*p* dangling-bond band is almost unaffected by surface relaxation. This is considered to arise from the fact that only the Zn 4*s* and O 2*p* orbitals were taken into account as a basis set in the calculations so that the ionic character of the Zn-O bonding is emphasized.<sup>7</sup> Meanwhile, Wang and Duke have used the *sp*<sup>3</sup> empirical tight-binding method, which includes the Zn 4*p* orbitals in addition to the Zn 4*s* and O 2*p* orbitals as the bases.<sup>5</sup> In the *sp*<sup>3</sup> model, covalency of the Zn-O bonding is stressed. As a result, the surface relaxation, which is characterized by a large Zn-O bond rotation with an rotation angle of 17° in the energy-optimized geometry, significantly modifies the dangling-bond states. On the ideal ZnO(10 $\bar{1}$ 0) surface, the *sp*<sup>3</sup> model predicts that the O 2*p* dangling-bond band locates within the bulk band gap above the projected bulk bands along the main high-symmetry axes of the surface Brillouin zone (BZ), i.e., the  $\bar{\Gamma}X$ ,  $\bar{\Gamma}X'$ ,  $XM$ , and  $MX'$  axes. However, the relaxation stabilizes the band by 0.4–0.9 eV so that a major part of the band shifts into the projected bulk-band region, and the gap state is predicted only along the  $\bar{MX}$  and  $\bar{MX}'$  axes.<sup>5</sup> Thus, although these two empirical tight-binding methods give different results on the degree of the relaxation-induced stabilization of the O 2*p* dangling-bond states, both predict that the O 2*p* dangling-bond band locates within the projected bulk-band region at least along the  $\bar{\Gamma}X$  and  $\bar{\Gamma}X'$  axes in their energy-optimized relaxed surfaces.

The first *ab initio* calculations of the ZnO(10 $\bar{1}$ 0) surface have been carried out by Schröer *et al.* utilizing the density-functional formalism within the local-density-functional approximation (LDA).<sup>6</sup> In their LDA calculations, the Zn<sup>12+</sup> ionic pseudopotential has been used, i.e., the Zn 3*d* electrons are treated as valence electrons. Although this results in the

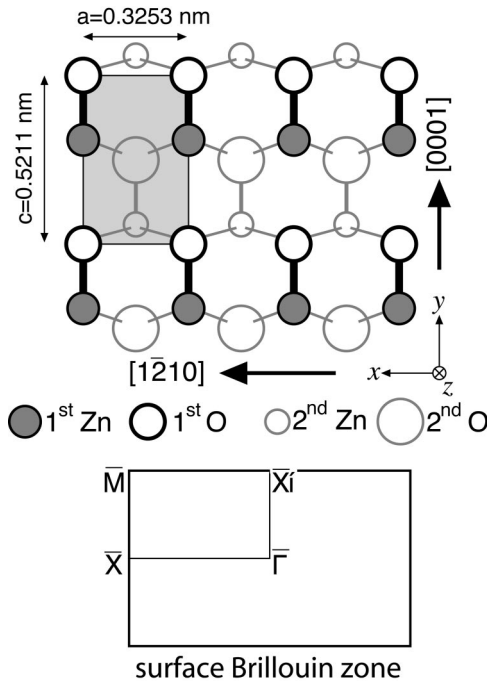


FIG. 1. A top view of the geometric structure of the ZnO( $10\bar{1}0$ ) surface. In the angle-resolved photoelectron spectroscopy (ARPES) measurements, the incidence plane of the light was parallel to the  $[1\bar{2}10]$  direction, and the photoelectrons were detected in the planes parallel to the  $[1\bar{2}10]$  or  $[0001]$  directions. The surface Brillouin zone is shown in the lower part.

narrowing of the valence-band width by  $\sim 3$  eV compared with the experimental result,<sup>8</sup> the upper region of the calculated bulk-band structure is found to resemble those given by the empirical tight-binding methods.<sup>5,7</sup> Schröer *et al.* have shown that the O  $2p$  dangling-bond band on the ( $10\bar{1}0$ ) surface exists within the fundamental band gap along the  $\bar{\Gamma}X$ ,  $\bar{\Gamma}X'$ ,  $\bar{X}M$ , and  $\bar{M}X'$  axes even in the energy-optimized relaxation geometry (the Zn-O bond rotation angle of  $3.6^\circ$ ).<sup>6</sup> This result is in sharp contrast to those obtained from the above-mentioned empirical tight-binding approaches. Thus, it is still an open question as to the energetic position of the O  $2p$  dangling-bond band with respect to the projected bulk bands on the ZnO( $10\bar{1}0$ ) surface, and therefore the experimental study is highly desirable to settle the controversy about such a fundamental question.

Angle-resolved photoelectron spectroscopy (ARPES) is a powerful tool to investigate both bulk and surface valence electronic structures of metal and semiconductor crystals.<sup>9</sup> The first detailed ARPES study applied to the ZnO( $10\bar{1}0$ ) surface has been carried out by Göpel *et al.*<sup>10</sup> They have identified two surface-induced features at the  $\bar{\Gamma}$ ,  $\bar{M}$ , and  $\bar{X}$  points of the surface BZ and have assigned these states to the O  $2p$ -derived dangling-bond state and the Zn-O backbond state.<sup>10</sup> Nevertheless, detailed discussions on the two-dimensional band structure of these surface related states have not been given in Ref. 10. Zwicker and Jacobi have also performed the ARPES study on the ZnO( $10\bar{1}0$ ) surface<sup>11</sup>

and have revealed the valence-band structure along the  $\bar{\Gamma}M$  axis of the bulk BZ. In this experiment, however, a surface related state is not identified and all the observed peaks are attributed to the bulk-band transitions.

In the present study, we performed the ARPES measurements to investigate the two-dimensional band structure of the O  $2p$  dangling-bond state on the ZnO( $10\bar{1}0$ ) surface along the selected high-symmetry axes of the surface BZ, i.e., the  $\bar{\Gamma}X$  and  $\bar{\Gamma}X'$  axes. The energetic position relative to the projected bulk bands and the dispersion width of the dangling-bond band are determined and are compared with the calculated band structures by Wang and Duke<sup>5</sup> and by Schröer *et al.*<sup>6</sup>

## II. EXPERIMENT

The ARPES measurements were performed at Beam Line 11C of the Photon Factory, High Energy Accelerator Research Organization (KEK), where synchrotron light was dispersed by a Seya-Namioka monochromator. Photoelectrons were collected by an electron energy analyzer of the  $180^\circ$  hemispherical-sector type with an acceptance angle of  $\pm 1^\circ$ . The total experimental resolution was 0.25 eV at photon energy  $h\nu$  of 22.5 eV, which was estimated from the Fermi edge of the spectra of the Ta sample holder. The base pressure of the ultrahigh vacuum system was  $2 \times 10^{-10}$  Torr. All the measurements were carried out at room temperature.

A ZnO crystal with the ( $10\bar{1}0$ ) orientation (MaTeck Co.) was set so that the incidence plane of the light was parallel to the  $[1\bar{2}10]$  direction, which corresponds to the direction perpendicular to the mirror plane of the ( $10\bar{1}0$ ) surface. The incidence light was linearly polarized in the incidence plane, and photoelectrons were detected in the incidence plane (parallel to the  $[1\bar{2}10]$  direction) or in the plane perpendicular to the incidence plane (parallel to the  $[0001]$  direction). The *in situ* preparation to remove surface contamination involved cycles of Ar<sup>+</sup> sputtering (2–3 kV, 0.5–1  $\mu$ A) and annealing at 1050 K for several times. Then, the sample was annealed at 700 K in O<sub>2</sub> atmosphere ( $3 \times 10^{-6}$  Torr) for 10 min to restore the surface stoichiometry. Finally, the surface was mildly annealed at 650 K to remove possible oxygen adsorbates. The clean surface thus prepared showed a sharp ( $1 \times 1$ ) LEED pattern.

In this paper, the incidence angle of the light,  $\theta_i$ , and the detection angle of the photoelectrons,  $\theta_d$ , are given relative to the surface normal. In the ARPES spectra presented below, the electron binding-energy is given relative to the Fermi level  $E_F$ , which is determined from the Fermi cutoff in the Ta spectra.

## III. RESULTS

Figure 2 shows a series of normal-emission spectra of the clean ZnO( $10\bar{1}0$ ) surface taken at photon energies between 17 and 27 eV. A peak at 10–11 eV is associated with the emission from the Zn  $3d$  levels. The peak is symmetric in the spectra taken at  $h\nu=20$  and 21 eV, whereas a shoulder structure becomes obvious in the higher binding-energy side

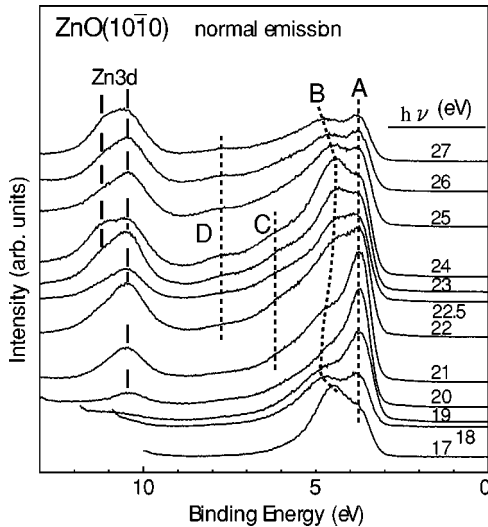


FIG. 2. Normal-emission spectra of ZnO( $10\bar{1}0$ ) as a function of photon energy. The incidence angle of the light was  $45^\circ$ . The peak positions were determined by taking the second derivative of the measured spectra so that the peak maxima were enhanced.

at  $h\nu \geq 22$  eV. The second derivative of the observed spectra clarifies the positions of the Zn  $3d$  peaks, and they are indicated by vertical bars. The main peak lies at 10.4 eV, while the shoulder peak appears at 11.2 eV. Such a double-peak structure of the Zn  $3d$  emission peak is also observed in the earlier ARPES studies by Zwicker and Jacobi for the ( $10\bar{1}0$ ) surface<sup>11</sup> and by Girard *et al.* for the (0001) surface,<sup>12</sup> and, from the LDA calculations, it is interpreted to be due to the splitting of ten Zn  $3d$  bands into two subgroups with four and six bands induced by a strong Zn  $3d$ -O  $2p$  interaction.<sup>8</sup>

In the energy region between 3 and 8 eV, where the valence bands composed mainly of the O  $2p$  orbitals with minor contribution of the Zn  $4sp$  and/or  $3d$  orbitals are formed, four peaks are observed and are labeled as A–D. The peak positions are determined from the second derivative of the spectra and are indicated by dashed curves. Of these four peaks, only peak B has an apparent dispersive feature in the binding-energy region between 4 and 5 eV. This is a typical behavior of a direct transition from a bulk valence band. Other three peaks (A, C, and D at 3.7, 6.2, and 7.8 eV, respectively), on the other hand, do not show a substantial shift as a function of  $h\nu$ . Such a nondispersive feature is interpreted to be due either to the emission from surface states or to the indirect bulk-band transition involving bands with a high density of states. In order to clarify the origin of these nondispersive features, we have carried out K and O<sub>2</sub> adsorption experiments. If peaks are associated with the states localized at the surface, they should be sensitive to chemisorption of atoms or molecules. Figure 3(a) shows the normal- ( $\theta_d=0^\circ$ ) and off-normal- ( $20^\circ$ ) emission spectra of the clean and K-adsorbed ZnO( $10\bar{1}0$ ) surfaces. It is obvious that lowest-lying peak A is leadingly quenched compared with other peaks as the surface is being covered with K for both detection geometries (peak C cannot be identified in the second derivative of these spectra, probably due to a small cross-section of this state in this detection geometry). Simi-

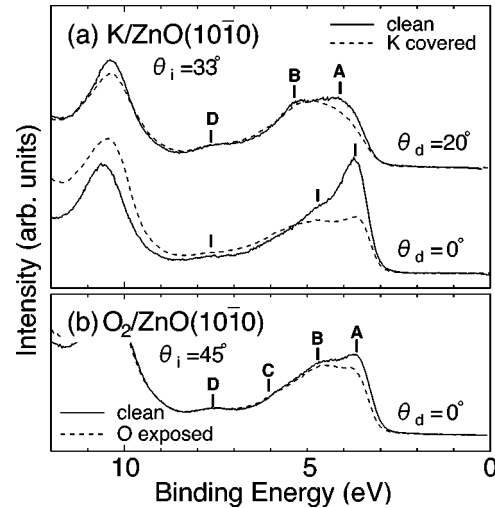


FIG. 3. (a) Angle-resolved photoelectron spectra at two different detection angles for clean (solid lines) and K-covered (dashed lines) ZnO( $10\bar{1}0$ ) surfaces. The incidence angle of the light  $\theta_i$  was  $33^\circ$  and photon energy  $h\nu$  used was 20 eV. The K coverage was estimated to be  $(3.6 \pm 0.9) \times 10^{14} \text{ cm}^{-2}$ , which corresponds to  $72 \pm 17\%$  of the saturation coverage. (b) Normal-emission spectra for the clean and 1000-L O<sub>2</sub>-exposed surfaces (1 L =  $1 \times 10^{-6}$  Torr s). The photon energy used was 20 eV and  $\theta_i$  was  $45^\circ$ .

larly, oxygen adsorption attenuates the intensity of peak A, while peaks B–D are not affected much as shown in Fig. 3(b). Therefore, peak A can be assigned to the emission from the surface-localized states, whereas peaks C and D are related to the bulk-band emission. It is worth noting that, on ZnO(0001), the dispersionless features as a function of  $h\nu$  have also been observed in the same binding-energy regions as those of peaks C and D; one lies at  $\sim 6$  eV and the other at 7–8 eV.<sup>12</sup> These are interpreted to arise from indirect transition processes from high densities of states formed just above the large bulk-band gap at 6–7 eV and at the bottom of the bulk valence bands (7–8 eV).<sup>12</sup> On the ( $10\bar{1}0$ ) surface, a large gap is also expected at 6–7 eV in the projected bulk band at around the  $\bar{M}$  point of the surface BZ, and the bottom of the valence band lies at  $\sim 8$  eV.<sup>7,5,6</sup> Thus, we attribute peaks C and D to the emission from the bulk valence bands with high densities of states.

The theoretical studies have indicated that the anion-derived dangling-bond state is formed on the ( $10\bar{1}0$ ) surfaces of wurtzite II-VI semiconductors as well as isolectric III-V semiconductors near the top of the valence bands.<sup>5–7,13–16</sup> Such a state has been experimentally identified by ARPES at  $\sim 4$  eV below  $E_F$  on ZnO( $10\bar{1}0$ ),<sup>10</sup> in good agreement with the position of peak A. Considering that peak A is associated with the surface-related state because of its sensitiveness to K and O<sub>2</sub> adsorption, it can be assigned to the emission from the O  $2p$  dangling-bond state.

Figure 4 shows off-normal-emission spectra taken at various detection angles along the  $[\bar{1}2\bar{1}0]$  ( $\bar{\Gamma}X$ ) and  $[0001]$  ( $\bar{\Gamma}X'$ ) azimuths. A set of the spectra for both directions bears four peaks at 3–8 eV corresponding to peaks A–D in Fig. 2.

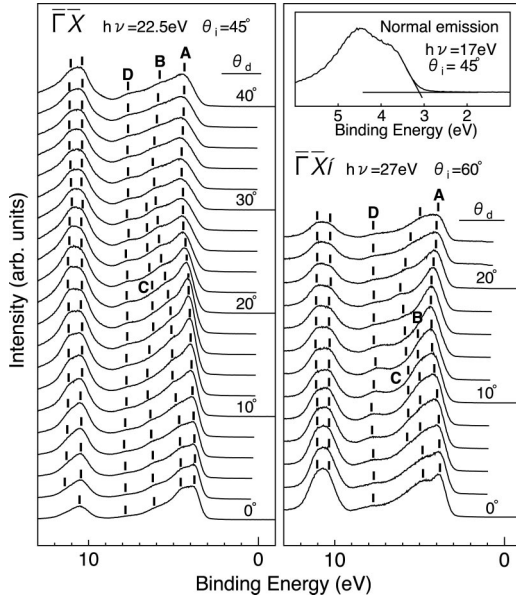


FIG. 4. Off-normal emission spectra of the clean surface recorded at  $h\nu=22.5$  eV and  $\theta_i=45^\circ$  along the  $[1\bar{2}10]$  ( $\Gamma\bar{X}$ ) direction and at  $h\nu=27$  eV and  $\theta_i=60^\circ$  along the  $[0001]$  ( $\Gamma X'$ ) direction. The incidence plane of the light was parallel to the  $[1\bar{2}10]$  direction for both detection directions. The spectra are shown with  $2^\circ$  interval. Peak positions, indicated by vertical bars, were determined from the second derivative of the spectra. The position of the valence band maximum was determined from the normal-emission spectrum taken at  $h\nu=17$  eV by extrapolating the onset of the valence-band emission as shown in the inset of the right panel.

Peak *D* does not show an appreciable dispersion as  $\theta_d$  varies. The position of peak *C*, on the other hand, depends on  $\theta_d$ , having a rather complex dispersion. Peak *B* shifts monotonically to the higher binding-energy side from 4.6 eV at  $\theta_d=0^\circ$  to 6.2 eV at  $33^\circ$ , which corresponds to the boundary of the surface BZ in the  $\Gamma\bar{X}$  axis, and to 5.1 eV at  $12^\circ$  along the  $\Gamma X'$  direction. The O  $2p$  dangling-bond state *A* also moves to the higher binding-energy side as  $\theta_d$  increases in both directions. The two-dimensional band structure of the O  $2p$  dangling-bond state can be mapped using a relation between the parallel component of the wave vector  $k_{\parallel}$  and the measured binding-energy  $E_B$ , i.e.,  $k_{\parallel} = \sqrt{2m_e(h\nu - \Phi - E_B)/\hbar^2} \sin \theta_d$ , where  $m_e$  is the mass of the electron and  $\Phi$  is the work function of the clean surface, which is determined to be 4.52 eV. The result is plotted in Fig. 5 by open circles. In Fig. 5, we also show the peak positions of peaks *B–D* as filled circles. The hatched area indicates the region of the bulk-bands projected onto the  $(10\bar{1}0)$  surface obtained from the theoretical study by Wang and Duke.<sup>17</sup> As indicated in the inset of the right panel of Fig. 4, the position of the valence-band maximum  $E_{\text{VBM}}$  was evaluated by taking a linear extrapolation of the onset of the valence-band emission in the normal-emission spectrum measured at  $h\nu=17$  eV.<sup>18</sup> The  $E_{\text{VBM}}$  value determined thus far is  $3.15 \pm 0.05$  eV below  $E_F$  at the  $\bar{\Gamma}$  point. From this, the electron affinity of the surface is calculated to be 4.37 eV,<sup>19</sup> which is in good agreement with that reported by Jacobi

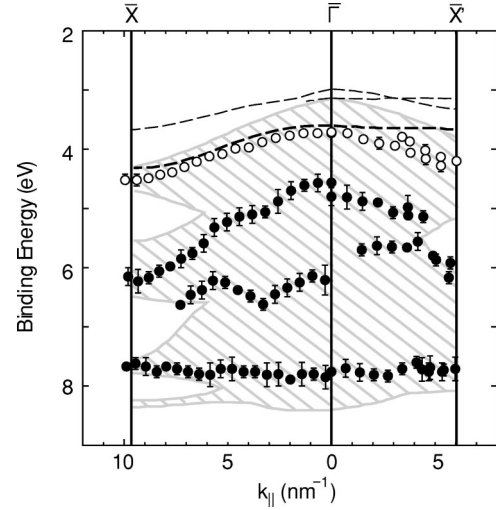


FIG. 5. Measured dispersion of the O  $2p$  dangling-bond state (open circle) and the bulk-band related states (filled circles) along the  $\Gamma\bar{X}$  and  $\Gamma X'$  axes. Hatched area corresponds to the projected bulk-band region and a bold dashed line indicates the O  $2p$  dangling-bond bands, both of which have been calculated using the  $sp^3$  model by Wang and Duke (Ref. 5). Thin dashed lines which locate above the projected bulk bands are the dangling-bond band obtained from the LDA calculations (Ref. 6).

*et al.* for the same surface.<sup>20</sup> Thus, the energy alignment in this way is rationalized. In Fig. 5, the calculated projected bulk-bands is, therefore, shifted vertically so that the valence-band maximum coincides with 3.15 eV below  $E_F$ .

Figure 5 shows that the O  $2p$  dangling-bond state positions at 3.7 eV at the  $\bar{\Gamma}$  point and shifts downwards by 0.5 eV up to the  $X'$  point, while the 0.8-eV shift is seen along the  $\Gamma\bar{X}$  direction. Along both directions, the dangling-bond band lies well below the upper edge of the projected bulk bands. It should be noted that, even if we employ the projected bulk bands given by Ivanov and Pollmann<sup>7</sup> or by Schröer *et al.*,<sup>6</sup> the dangling-bond band also locates within the projected bulk-band region along the  $\Gamma\bar{X}$  and  $\Gamma X'$  axes, since the dispersion widths of the upper edge of the projected bulk bands are 1.3 and 0.7 eV by Ivanov and Pollmann<sup>7</sup> and 0.9 and 0.4 eV by Schröer *et al.*<sup>6</sup> in the  $\Gamma\bar{X}$  and  $\Gamma X'$  axes, respectively, whereas those by Wang and Duke are 1.2 and 0.7 eV.<sup>5</sup> Bulk band *B* shifts to the higher binding-energy side towards both the  $X$  and  $X'$  points with a smaller dispersion along the  $\Gamma X'$  axis. Band *C* shows a rather complex dispersion in both directions. Band *D* form a flat band at  $\sim 7.7$  eV, which corresponds to  $\sim 4.6$  eV below  $E_{\text{VBM}}$ , in good agreement with the position of the peak (4.8 eV) in the bulk valence-band density of states calculated by Wang and Duke.<sup>5</sup>

#### IV. DISCUSSION

It is revealed from the present ARPES measurements that the O  $2p$  dangling-bond band on  $\text{ZnO}(10\bar{1}0)$  locates within the projected bulk-band region in both the  $\Gamma\bar{X}$  and  $\Gamma X'$  axes, i.e., the state is a surface resonance at least along these axes.

Although the band structure in other high-symmetry axes of the surface BZ has not been observed yet, the present result settles the controversial issue about the position of the occupied dangling-bond band relative to the projected bulk bands. The empirical tight-binding calculations done by Ivanov and Pollmann<sup>7</sup> and by Wang and Duke,<sup>5</sup> which emphasize the ionic and covalent characters of the Zn-O bonds, respectively, predict that the gap state by the O  $2p$  dangling bond is not formed at least in the  $\bar{\Gamma}X$  and  $\bar{\Gamma}X'$  axes. On the other hand, Schröer *et al.* have found in their LDA study that the dangling-bond band is formed within the gap above the upper edge of the projected bulk bands along the major high-symmetry axes of the surface BZ.<sup>6</sup> Therefore, the result obtained in the present study is consistent qualitatively with the band structure given by two empirical tight-binding approaches.

In the empirical approach by Ivanov and Pollmann, a pronounced surface resonance from the O  $2p$  dangling-bond state has not been found along the  $\bar{\Gamma}X$  and  $\bar{\Gamma}X'$  axes.<sup>7</sup> On the other hand, the empirical calculations using the  $sp^3$  model by Wang and Duke have predicted a surface resonance near the top of the valence bands along these axes. In Fig. 5, the O  $2p$  dangling-bond band by the  $sp^3$  model is shown by a bold dashed line<sup>5</sup> along with those obtained from the LDA calculations by Schröer *et al.*<sup>6</sup> by thin dashed lines. The energetic position of the observed dangling-bond band is in fair agreement with the calculated band by the  $sp^3$  model for both  $\bar{\Gamma}X$  and  $\bar{\Gamma}X'$  directions. The  $sp^3$  model predicts a band dispersion width of 0.7 eV along the  $\bar{\Gamma}X$  axis, and the agreement with the experimentally determined band structures is excellent. It should be noted that, although the energetic position of the dangling-bond band cannot be reproduced by the LDA calculations, the shape of the band resembles the experimentally determined one in the  $\bar{\Gamma}X$  axis so that a vertical shift of the calculated band by 0.6–0.7 eV to the higher binding-energy side leads to a satisfying agreement with the experimental result.

Along the  $\bar{\Gamma}X'$  axis, on the other hand, the  $sp^3$  model has given a flat dangling-bond band, whereas a band with a substantial dispersion (0.5 eV) is observed experimentally. Such a dispersive character of the O  $2p$  dangling-bond band along this axis is somewhat surprising, because a neighboring distance between the O atoms is relatively large in the [0001] direction (0.5211 nm). The dispersionless band by the  $sp^3$  model should reflect the large O-O distance in the [0001] direction, i.e., an interaction between the neighboring O  $2p$  dangling-bond orbitals should be small in this direction. However, experimentally determined band dispersion implies an appreciable interaction between the neighboring O  $2p$  dangling bonds in the [0001] direction, probably due to a stronger hybridization of the O  $2p$  orbitals with the Zn  $4sp$  and/or  $3d$  orbitals than that predicted by the band calculations using the  $sp^3$  model [the Zn  $4sp$  contribution is estimated to be  $\sim 10\%$  (Ref. 5)] so that the lateral interaction between the dangling-bond orbitals becomes large even in the [0001] direction. This hypothesis is partly supported by the LDA calculations, which give a band with a dispersive feature (0.3–0.4 eV) aside from a flat band along the  $\bar{\Gamma}X'$

direction (Fig. 5). The dispersive state is found to be composed of  $\sim 70\%$  of the O  $2p$  orbitals with  $\sim 30\%$  of the Zn  $3d+4p$  orbitals at the  $\bar{X}'$  point.<sup>6</sup> Thus, a substantial contribution of the Zn valence orbitals could be responsible for the observed dispersion of the dangling-bond band.

In the present ARPES study, we used the light polarized in the incidence plane, which is perpendicular to the mirror plane of the ZnO(10 $\bar{1}$ 0) surface, with an incidence angle  $\theta_i$  of  $60^\circ$ , and the photoelectrons were corrected in the plane parallel to the mirror plane for measuring the band structure along the  $\bar{\Gamma}X'$  axis. In such a geometry, all of the O  $2p_x$ -,  $2p_y$ -, and  $2p_z$ -derived dangling-bond bands are detected (here, the coordination system is chosen as indicated in Fig. 1), i.e., the states with both even and odd symmetry with respect to the mirror plane of the surface are observable. The LDA calculations have shown that there exist two dangling-bond bands with different dispersion behavior in the  $\bar{\Gamma}X'$  axis as shown in Fig. 5, and the flat and dispersive bands are classified as having even and odd symmetry, respectively.<sup>6</sup> However, the ARPES spectra show that only a single band with a dispersive character exits along the  $\bar{\Gamma}X'$  axis (see Fig. 4), although both even and odd bands are detectable under the present experimental condition. The lack of the theoretically predicted flat band in the ARPES spectra may be due to the lower cross section of the states with even symmetry compared with those with odd symmetry in the present experimental condition. In order to clarify more detailed band structures of the O  $2p$  dangling-bond states, symmetry resolved measurements should be required.

Finally, the anion-derived dangling-bond band on the ZnO(10 $\bar{1}$ 0) surface is compared with those on other wurtzite II-VI semiconductor surfaces. As far as we know, only the CdS and CdSe(10 $\bar{1}$ 0) surfaces have been studied utilizing the APRES.<sup>21,22</sup> On both surfaces, anion-derived dangling-bond bands are observed near the top of the valence bands, and the two-dimensional structures of these bands are similar to that on the ZnO(10 $\bar{1}$ 0) surface, i.e., the dangling-bond states shift downwards away from the  $\bar{\Gamma}$  point towards the  $\bar{X}$  and  $\bar{X}'$  points. The dispersion widths are 0.4 and 0.5 eV for CdS and CdSe, respectively, along the  $\bar{\Gamma}X'$  axis, whereas the 1-eV dispersion is observed for CdS along the  $\bar{\Gamma}X$  axis.<sup>21,22</sup> These dispersion widths are comparable to or larger than those on the ZnO surface, although the lattice constants are larger for CdS and CdSe than ZnO, suggesting the larger spatial extent of the anion dangling-bond orbitals on the CdS and CdSe surfaces than on the ZnO surface. Along the  $\bar{\Gamma}X$  and  $\bar{\Gamma}X'$  axes, the dangling-bond bands are found to locate within the projected bulk bands as in the case for the present system. However, Wang and Duke have shown in their theoretical study using the  $sp^3$  model that a part of the anion-derived dangling-bond bands disperses in the gap region in these two high-symmetry axes.<sup>15</sup> This discrepancy implies the insufficiency of the model calculations for CdS and CdSe, although it partially reproduces our experimental results for ZnO. Thus, further theoretical investigations beyond the empirical  $sp^3$  tight-binding model or the *ab initio* calculation within LDA as used by Schröer *et al.* should be needed

to consistently and systematically describe the experimentally determined band structures of the II-VI semiconductor surfaces including ZnO.

## V. SUMMARY

Anion-derived dangling-bond states on the ZnO(10 $\bar{1}$ 0) surface has been investigated by ARPES utilizing synchrotron radiation, and the band structure of the dangling-bond states along the selected high-symmetry axes of the surface BZ is determined experimentally. The O 2*p* dangling-bond state locates at 3.7 eV below  $E_F$  at the  $\bar{\Gamma}$  point and shifts to the higher binding-energy side by 0.8 and 0.5 eV towards the  $\bar{X}$  and  $\bar{X}'$  points, respectively. It is found that the valence-band maximum locates at  $3.15 \pm 0.05$  eV below  $E_F$  and that the O 2*p* dangling-bond band lies below the upper edge of

the projected bulk bands along  $\bar{\Gamma X}$  and  $\bar{\Gamma X}'$  axes, i.e., the band is a surface resonance along these high-symmetry axes. The present study settles a controversial issue on the energetic position of the O 2*p* dangling-bond band relative to the projected bulk bands, which has been inconsistent among theoretical studies.

## ACKNOWLEDGMENTS

This work was performed under the approval of the Photon Factory Advisory Committee (Proposal No. 2002G-009). We thank the staff of the Photon Factory for their excellent support. The work was financially supported by a Grants-in-Aid for Scientific Research (Contract No. 14740374) from the Ministry of Education, Culture, Sports, Science, and Technology of Japan.

\*Electronic address: kozawa@chem.titech.ac.jp

<sup>†</sup>Present address: Hiroshima Synchrotron Radiation Center, Hiroshima University, 2-313 Kagamiyama, Higashi-Hiroshima 739-8526, Japan.

<sup>1</sup>Y. Segawa, A. Ohtomo, M. Kawasaki, H. Koinuma, Z.K. Tang, P. Yu, and G.K.L. Wong, *Phys. Status Solidi B* **202**, 669 (1997).

<sup>2</sup>D.M. Bagnall, Y.F. Chen, Z. Zhu, T. Yao, S. Koyama, M.Y. Shen, and T. Goto, *Appl. Phys. Lett.* **70**, 2230 (1997).

<sup>3</sup>C.B. Duke, A.R. Lubinsky, S.C. Chang, B.W. Lee, and P. Mark, *Phys. Rev. B* **15**, 4865 (1977).

<sup>4</sup>C.B. Duke, R.J. Meyer, A. Paton, and P. Mark, *Phys. Rev. B* **18**, 4225 (1978).

<sup>5</sup>Y.R. Wang and C.B. Duke, *Surf. Sci.* **192**, 309 (1987).

<sup>6</sup>P. Schröer, P. Krüger, and J. Pollmann, *Phys. Rev. B* **49**, 17 092 (1994).

<sup>7</sup>I. Ivanov and J. Pollmann, *Phys. Rev. B* **24**, 7275 (1981).

<sup>8</sup>P. Schröer, P. Krüger, and J. Pollmann, *Phys. Rev. B* **47**, 6971 (1994).

<sup>9</sup>*Angle Resolved Photoemission*, edited by S. D. Kevan (Elsevier, Amsterdam, 1991).

<sup>10</sup>W. Göpel, J. Pollmann, I. Ivanov, and B. Reihl, *Phys. Rev. B* **26**, 3144 (1982).

<sup>11</sup>G. Zwicker and K. Jacobi, *Solid State Commun.* **54**, 701 (1985).

<sup>12</sup>R.T. Girard, O. Tjernberg, G. Chiaia, S. Söderholm, U.O. Karlsson, C. Wigren, H. Nylén, and I. Lindau, *Surf. Sci.* **373**, 409 (1997).

<sup>13</sup>Y.R. Wang and C.B. Duke, *Phys. Rev. B* **36**, 2763 (1987).

<sup>14</sup>Y.R. Wang, C.B. Duke, and C. Mailhot, *Surf. Sci.* **188**, L708

(1987).

<sup>15</sup>Y.R. Wang and C.B. Duke, *Phys. Rev. B* **37**, 6417 (1988).

<sup>16</sup>A. Filippetti, V. Fiorentini, G. Cappellini, and A. Bosin, *Phys. Rev. B* **59**, 8026 (1999).

<sup>17</sup>Although the theoretically derived band structure of the O 2*p* dangling bond is largely dependent on the method employed, i.e., two types of the empirical tight-binding calculations (Refs. 5,7) and the LDA calculation (Ref. 6), the calculated bulk-band structures are almost identical among them especially at the upper part of the valence band. Thus, the upper part of the projected bulk bands also resembles among these three.

<sup>18</sup>The use of the normal-emission spectrum measured at  $h\nu = 17$  eV is because the energy region around the onset of the valence bands ( $\sim 3$  eV) corresponds nearly to the  $\Gamma$  point of the bulk BZ, where the bulk valence-band reaches the maximum. In order to determine the normal component of the wave vector, we used the inner potential of 9.8 eV, which was determined for the same surface by Zwicker and Jacobi (Ref. 11).

<sup>19</sup>The electron affinity  $\chi$  is calculated by the following equation;  $\chi = \Phi + (E_{\text{VBM}} - E_F) - E_g$ , where  $E_g$  is the band-gap of ZnO,  $3.3 \pm 0.1$  eV.

<sup>20</sup>K. Jacobi, G. Zwicker, and A. Gutmann, *Surf. Sci.* **141**, 109 (1984).

<sup>21</sup>K.O. Magnusson, S.A. Flodström, P. Mårtensson, J.M. Nicholls, U.O. Karlsson, R. Engelhardt, and E.E. Koch, *Solid State Commun.* **55**, 643 (1985).

<sup>22</sup>K.O. Magnusson and S.A. Flodström, *Phys. Rev. B* **38**, 6137 (1988).